search in Industry and Agriculture (I.W.O.N.L.). The help of Dr. F. C. Mijlhoff and Ing. G. Renes (University of Leiden, the Netherlands) during the experimental part of the investigation is gratefully acknowledged. Support of the University of Arkansas computing center in executing the ab initio calculations is gratefully acknowledged.

Supplementary Material Available: List of values of intensity (I), background (B), $1 + M_{obsd}$, and $1 + RM_{calcd}$ as a function of s for three s regions, and Cartesian coordinates of the refined ab initio structures of the syn, skew, and anti forms (3 pages). Ordering information is given on any current masthead page.

References and Notes

(1) (a) University of Antwerp; (b) University of Arkansas.
(2) (a) K. Kuchitsu in "Molecular Structures and Vibrations", S. J. Cyvin, Ed., Elsevier, Amsterdam, 1972, Chapter 12; (b) K. Kuchitsu and K. Oyanagi, *Faraday Discuss. Chem. Soc.*, **62**, 20 (1977).
(3) N. S. Chiu, H. L. Sellers, and L. Schäfer, *J. Am. Chem. Soc.*, in press.
(4) S. Kondo, E. Hirota, and Y. Morino, *J. Mol. Spectrosc.*, **28**, 471 (1968).
(5) O. Ermer and S. Lifson, *Tetrahedron*, **30**, 2425 (1974).
(6) A. J. Barnes and J. D. R. Howells, *J. Chem. Soc., Faraday Trans. 2*, **69**, 532 (1973).
(7) P. B. Woller and E. W. Garbisch Jr., *J. Org. Chem.*, **37**, 4281 (1972).
(8) F. H. A. Rummens, *J. Magn. Reson.*, **6**, 550 (1972).
(9) J. W. De Haan, L. J. M. Van de Ven, A. R. N. Wilson, A. E. Van der Hout-Lodder, C. Altona, and D. H. Faber, *Org. Magn. Reson.*, **8**, 477 (1976).
(10) H. R. Foster, *J. Appl. Phys.*, **41**, 5344 (1970).
(11) K. Tamagawa, T. Iijima, and M. Kimura, *J. Mol. Struct.*, **30**, 243 (1976).
(12) L. Van den Enden, E. Van Laere, H. J. Geise, F. C. Mijlhoff, and A. Spelbos, *Bull. Soc. Chim. Belg.*, **85**, 735 (1976).
(13) These data have been deposited as supplementary material.
(14) O. Ermer and S. Lifson, *J. Am. Chem. Soc.*, **95**, 4121 (1973).
(15) H. L. Sellers and L. Schäfer, *J. Mol. Struct.*, **51**, 117 (1979).
(16) I. Tokue, T. Fukuyama, and K. Kuchitsu, *J. Mol. Struct.*, **17**, 207 (1973).
(17) P. Pulay, *Mol. Phys.*, **17**, 197 (1969).
(18) P. Pulay, G. Fogarasi, F. Pang, and J. E. Boggs, *J. Am. Chem. Soc.*, **101**, 2550 (1979).
(19) H. L. Sellers, V. J. Klimkowski, and L. Schäfer, *Chem. Phys. Lett.*, **58**, 541 (1978).
(20) R. Ditchfield, W. J. Hehre, and J. A. Pople, *J. Chem. Phys.*, **54**, 724 (1971).
(21) I. Tokue, T. Fukuyama, and K. Kuchitsu, *J. Mol. Struct.*, **23**, 33 (1974).

Molecular Dynamics of Cis-Trans Isomerization in Rhodopsin

Robert R. Birge* and Lynn M. Hubbard[1]

Contribution from the Department of Chemistry, University of California, Riverside, California 92521. *Received August 8, 1979.*

Abstract: The photochemical properties of the chromophore in the visual pigment rhodopsin are analyzed using INDO-CISD molecular orbital theory and semiempirical molecular dynamics procedures. The molecular orbital calculations, which include restricted single and double excitation configuration interaction, predict a barrierless first excited singlet state potential surface for cis-trans isomerization of the protonated Schiff base chromophore. The molecular dynamics calculations predict that the excited-state species is trapped during isomerization in an activated complex which has a lifetime of ~0.5 ps. This activated complex rapidly oscillates between two components which preferentially decay to form isomerized product (bathorhodopsin) or unisomerized 11-cis chromophore (rhodopsin) within 1.9–2.3 ps. The nature of this activated complex virtually guarantees a quantum yield greater than 0.5 (our calculations predit a quantum yield of 0.57–0.61). Conformational distortion of the lysine residue is predicted to distort the chromophore in bathorhodopsin, preventing it from reaching a planar all-trans conformation. The molecular orbital calculations suggest that the conformational distortion will be concentrated in the C_7–C_{10} and/or C_{12}–C_{15} regions of the chromophore. Bathorhodopsin is predicted to have a free energy approximately 14 kcal/mol higher than that of rhodopsin due to compression of the lysine residue. The presence of a counterion near the C_{15}=N_{16} group in rhodopsin will increase the free energy of bathorhodopsin by ~12 kcal/mol to yield a relative bathorhodopsin free energy of ~26 kcal/mol above rhodopsin (neglecting the effect of other counterions). The bathochromic shift of the absorption maximum of bathorhodopsin relative to rhodopsin is attributed to the effects of the counterion as well as conformational distortion of the chromophore. We conclude that the classical concept that the chromphore in bathorhodopsin has a distorted all-trans geometry is the most realistic model for the first intermediate in the bleaching cycle of rhodopsin.

I. Introduction

The nature of the primary event in vertebrate vision is currently a subject of debate.[2-17] The controversy is focused on the characterization of the first intermediate in the visual cycle, bathorhodopsin (formerly called prelumirhodopsin), and arises from the belief of many investigators that the observed formation time of bathorhodopsin is too fast (<6 ps) to accommodate a 11-cis to 11-trans isomerization of the retinyl polyene.[11-16] Accordingly, a number of alternative mechanisms of bathorhodopsin formation have been proposed which involve proton translocation,[11-16] concerted multibond isomerization,[10] or photochemically induced charge reorganization which results in a trapped (stabilized) protein-chromophore complex.[17] Although all of these mechanisms allow for a rapid (<6 ps) transformation, none adequately accounts for the photochemical equilibrium which can be established among rhodopsin (11-cis), bathorhodopsin, and isorhodopsin (9-cis).

It was, in fact, the observation of the above photoequilibrium that prompted the early suggestion that bathorhodopsin is formed via a cis-trans isomerization yielding a chromophore with an all-trans conformation.[18] This assumption is further supported by the observation that metarhodopsin I, which is known to have an all-trans chromophore, can be photochemically reverted to both rhodopsin and isorhodopsin.[4,19]

This paper reinvestigates the classical picture of the initial step in visual transduction. We demonstrate, using semiempirical all-valence-electron molecular orbital theory and molecular dynamics, that a one-bond photochemical cis-trans isomerization can occur with high quantum efficiency in approximately 2 ps. The molecular orbital calculations, which include restricted single and double excitation configuration interaction, predict a barrierless first excited singlet state potential surface for cis-trans isomerization of the 11-cis protonated Schiff base. The mixing of covalent character into the principally ionic lowest $\pi\pi^*$ singlet state during isomerization

0002-7863/80/1502-2195$01.00/0

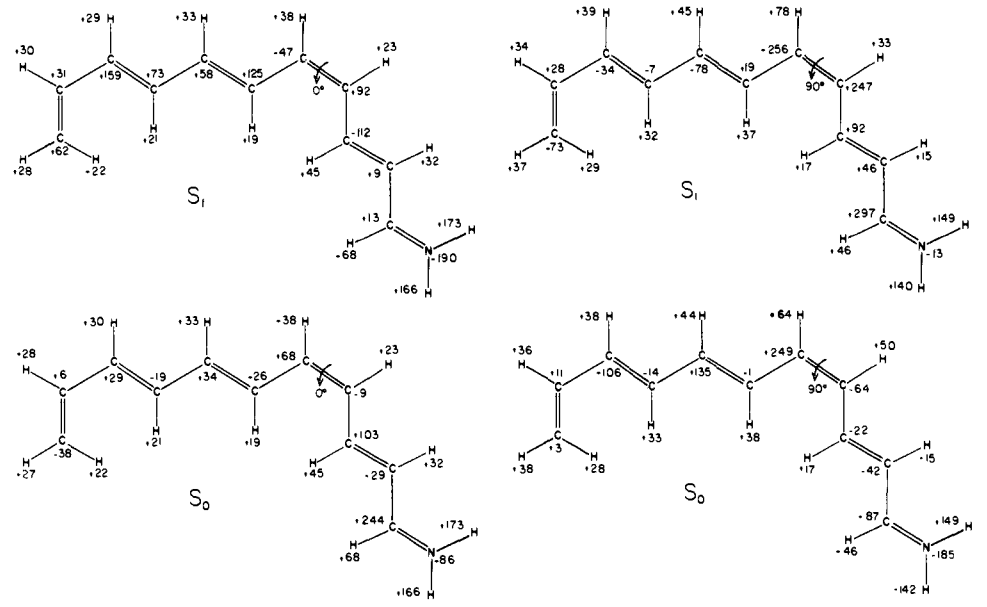

Figure 1. INDO-CISD atomic charges (electron units $\times 10^3$) in the 11-cis (planar) and 11,12-orthogonal (90°) conformations of the ground (S_0) and first excited $\pi\pi^*$ singlet (S_1) states of the protonated Schiff base of retinal. Mataga repulsion integrals, Sichel and Whitehead core parameters, and standard geometries were used (see text). The CI basis set included the lowest ~130 single excitations and the lowest ~260 double excitations.

produces a steep potential well with an energy minimum at an orthogonal 11,12 dihedral angle ($\theta_{11,12} = 90°$).[20] The molecular dynamics calculations predict that this potential well traps an activated complex which rapidly oscillates (4×10^{12} Hz) between excited-state conformations which preferentially decay to form all-trans product or 11-cis reactant. A quantum yield for isomerization of ~0.6 is calculated, in good agreement with observation. We demonstrate that most solution environments will significantly decrease both the quantum yield and rate of photochemical isomerization. Furthermore, we discuss possible mechanisms through which the opsin protein environment can influence the quantum yield and molecular dynamics of cis-trans isomerization. We conclude that the classical concept that the chromophore in bathorhodopsin has a distorted all-trans geometry is the most realistic model for the first intermediate in the bleaching cycle of rhodopsin.

II. Molecular Orbital Calculations

Numerous investigations of the visual chromophores using molecular orbital theory have been published.[10,16,17,21-37] However, the vast majority of these investigations have used restricted (π-electron) basis set procedures[10,21-33] which require rather severe, ad hoc assumptions concerning the core parameters of the nitrogen in protonated Schiff base compounds.[38] Potential inconsistencies in the standard parametrization approaches have been discussed in ref 21b. These parametrization problems, coupled with the inability of the PPP formalism to account for conformationally dependent polarization of the σ framework, prompted our use of the all-valence-electron INDO-CISD molecular orbital procedure for the present analysis.[39]

Our INDO-CISD formalism is modeled after the CNDO/S procedures of Del Bene and Jaffe.[40] The salient modifications which we have adopted include the use of one-center exchange integrals, Mataga repulsion integrals,[41] the one-center repulsion and core parameters of Sichel and Whitehead,[42] and a configuration interaction basis set including both single and double excitation CI.[39] The importance of including double CI for calculating the excited-state properties of the visual chromophores has been discussed in detail in the literature.[21-23,43,44]

All single excitations below 12 eV were included. The lowest energy N_{dble} double excitations were chosen to satisfy the equation $N_{dble} = K_{ds}N^0_{dble}(N_{sngl}/N^0_{sngl})$ where N^0_{sngl} and N^0_{dble} are the total number of possible single and double excitations,[45] N_{sngl} is the number of single excitations determined by the energy cutoff (see above), and K_{ds} is a constant empirically chosen to properly order covalent and ionic states. K_{ds} was adjusted to best fit the experimental "$^1A_g{}^{*-}$" – "$^1B_u{}^{*+}$" splitting in *all-trans*-retinol[22] and *all-trans*-retinal.[46] The Mataga two-electron repulsion integrals used for the retinal calculations require a value of 0.0043 for K_{ds}, yielding approximately 130 single and 260 double excitations for the truncated chromophore used in our calculations (see below).

Since a calculation of this type would be computationally intractable if the entire molecular framework of the retinyl chromophore were included, we approximate the PSB of retinal using a $C_{11}NH_{14}$ moiety (see Figure 1). A standard geometry was assumed for all of the calculations [$R_{C=C}$ = 1.35 Å, R_{C-C} = 1.46 Å, R_{C-H} = 1.08 Å, $R_{C=N}$ = 1.296 Å, R_{N-H} = 1.296 Å, R_{N-H} = 1.20 Å, all bond angles 120°, all dihedral angles planar trans (180°) except $\theta_{6,7}$, which is s-cis (45°), and $\theta_{11,12}$, which is variable[20]]. (It should be noted that the trajectory calculations include the inertial effects of the complete molecular framework of the chromophore including the β-ionylidene ring as well as the hydrocarbon chain of the lysine residue.)

The atomic charge distributions in the ground and first excited state for the planar 11-cis and partially isomerized ($\theta_{11,12}$ = 90°) geometries are shown in Figure 1. It is interesting to note that the nitrogen retains a negative charge despite the fact that the chromophore carries a net positive charge.[47] [This result suggests that the common approach of assigning nitrogen a +1 core charge in PPP calculations on protonated Schiff bases will overestimate the σ potential.[47] Note that the C_{15} Schiff base carbon is more positively charged than either the nitrogen atom or the proton in the 11-cis ground state (Figure 1).] Excitation to the first Franck-Condon excited state produces a more negatively charged nitrogen, which suggests that the proton is more tightly bound in the excited state. (However, we do not subscribe to the suggestion[11-16] that the Schiff base proton is translocated toward nitrogen in going from rhodopsin to bathorhodopsin.)

Sudden Polarization of Charge during Isomerization. Salem and Bruckmann recently proposed that the formation of a

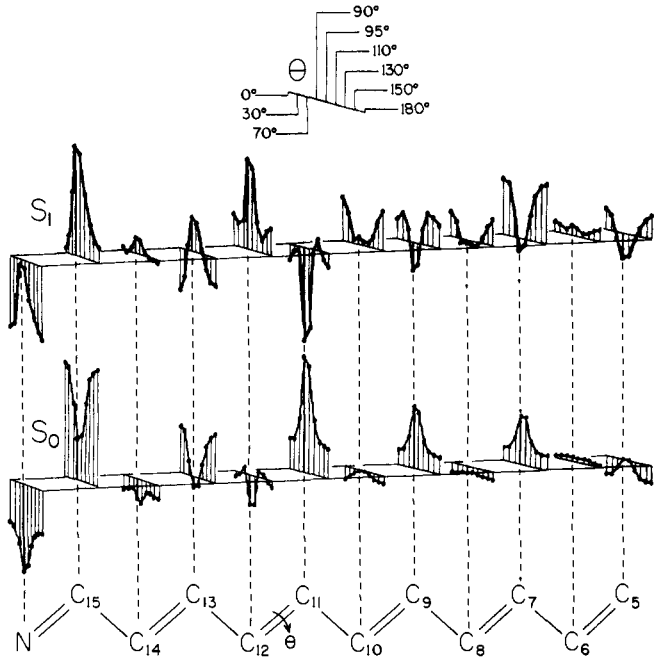

Figure 2. INDO-CISD atomic charges of the protonated Schiff base of retinal in the ground and first excited $\pi\pi^*$ singlet states graphed as a (discontinuous) function of the C_{11}–C_{12} dihedral angle. The dihedral angles, θ, associated with the vertical lines are assigned in the inset at the top of the figure. Positive charges are plotted (linearly) above the plane; negative changes are plotted below the plane. Note that the dihedral angle is not plotted linearly, $\theta = 0°$ is 11-cis (planar), and the atom numbers are assigned based on the standard convention for retinyl polyenes (e.g., Figure 3 of ref 23). Calculational details are defined in the caption to Figure 1.

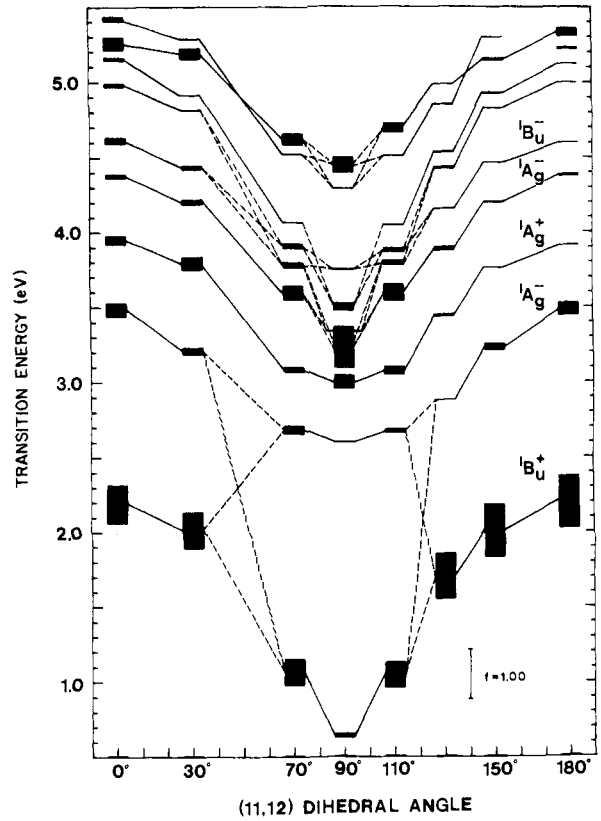

Figure 3. INDO-CISO transition energies and oscillator strengths in the protonated Schiff base of retinal as a function of C_{11}–C_{12} dihedral angle. The individual states are indicated by rectangular boxes and the height is proportional to the oscillator strength. Solid lines are used to connect states with the same symmetry and dashed lines are used to indicate significant state mixing. The symmetry labels are very approximate (see text).

nerve impulse in the visual transduction cycle of rhodopsin might be associated with a sudden polarization of the chromophore during isomerization.[36,37] Although we have reservations that such a short-lived event could be responsible for altering the polarization of the entire rod outer segment,[36,37] the dramatic changes in charge distribution calculated by these investigators may be important in directing the course of the isomerization. For example, electrostatic interactions between the chromophore and the protein could significantly alter the potential surface (see below).

The ab initio calculations of Salem and Bruckmann were carried out on a truncated pentadienyl chromophore and were followed by a 3 × 3 configuration interaction treatment.[36] Our semiempirical calculations include the entire π-electron system and a more complete single and double CI basis set. It is therefore interesting to compare the energies and charge distributions predicted by these two, significantly different molecular orbital formalisms.

INDO-CISD atomic charges in the ground and first excited singlet state are displayed as a function of 11,12 dihedral angle in Figure 2. The individual graphs for the various atoms indicate that the polarization of the atomic charges, which displays a maximum at an orthogonal 11,12 geometry ($\theta_{11,12} = 90°$), is a relatively smooth function of dihedral angle. The INDO-CISD and ab initio calculations[36,37] are in general agreement on this prediction.

However, the INDO-CISD calculations predict that the polarization of charge occurs in an opposite direction to that predicted by the ab initio calculations. As shown in Figures 1 and 2, the INDO-CISD procedures predict that a positive charge of 1.07 (electron charge units) is directed into the C_{12}–N_{16} moiety in the orthogonal first excited state with a concomitant −0.07 charge remaining in the C_5–C_{11} fragment. The ab initio calculations predict virtually the same magnitude of charge separation but place the positive charge in the C_7–C_{11} fragment. (Note that the C_5=C_6 double bond was not included in the ab initio treatment.[36]) The two procedures calculate an opposite polarization in the ground state relative to that in the excited state.

The origin of the difference in calculated polarization directions between the two formalisms is not clear. Similar discrepancies among different formalisms have been observed before,[37] and it is worth noting that extended basis set ab initio calculations have occasionally reversed the sign of the polarization relative to limited basis set calculations.[37] The fact that we have adopted a 12-s-trans geometry (Salem and Bruckmann studied a 12-s-cis geometry), included the entire π system, and followed the SCF calculation with a restricted single and double CI treatment may individually, or in total, be responsible for the INDO-CISD procedures prediction of a different polarization direction relative to Salem and Bruckmann's ab initio calculation.

INDO-CISD Transition Energies. INDO-CISD transition energies calculated as a function of C_{11}–C_{12} dihedral angle are displayed in Figure 3. The symmetry labels are very approximate and are derived by correlating the properties of a given electronic state with those of the analogous state in a linear polyene of C_{2h} symmetry.[20-23] Two-photon spectroscopy has recently demonstrated that the "$^1A_g{}^{*-}$" covalent state is the lowest lying $\pi\pi^*$ singlet state in *all-trans*-retinol[22] and *all-trans*-retinal.[46] Our INDO-CISD procedures were parametrized to properly order the "$^1A_g{}^{*-}$" state and the strongly allowed "$^1B_u{}^{*+}$" state in these two compounds (see above). Protonation of the Schiff base of retinal, however, is predicted to invert these two excited states by slightly destabilizing the covalent "$^1A_g{}^{*-}$" state and strongly stabilizing the ionic "$^1B_u{}^{*+}$" state.[23] Although there has been no direct spectro-

scopic confirmation of this level inversion, both the INDO-CISD and PPP-CISD procedures[23] predict that this inversion should take place, and there is ample spectroscopic evidence to support the bathochromic shift of the strongly allowed "$^1B_u{}^{*+}$" state upon protonation.

The absorption maximum of bovine rhodopsin is observed at 2.49 eV (497 nm) with an oscillator strength of approximately 0.8. The INDO-CISD calculations on the *isolated* protonated Schiff base of 11-*cis*, 12-*s*-*trans*-retinal shown in Figure 3 predict an absorption maximum at 2.20 eV (563 nm) with an oscillator strength of 0.73. The calculated oscillator strength would increase to 0.82 if the observed transition energy were used instead of the calculated transition energy [0.82 = (2.48/2.20)0.73] so the fact that the calculation underestimates the oscillator strength is due primarily to the error in the calculated transition energy.

We attribute the tendency of the INDO-CISD procedures to underestimate the transition energy to our neglect of environmental effects, in particular the neglect of counterions or negatively charged groups in the vicinity of the protonated imino nitrogen. The presence of a counterion near the nitrogen atom will blue shift the ΔE_{max}.[16,24-29] (The effects that a counterion will have on the photochemical properties of rhodopsin are examined below.) In solution, the counterion is expected to migrate to a minimum energy position in close proximity to the imino nitrogen. The absorption maximum of a retinal PSB chromophore in solution is observed at ~440 nm.[48] The bathochromic shift that accompanies the incorporation of the chromophore into the opsin protein may be primarily associated with constraints placed on the counterion by the geometry of the active site. We will subsequently demonstrate that placing a carboxylate anion approximately 3 Å from both the C_{15} and N_{16} atoms will produce a blue shift in the INDO-CISD λ_{max} to 475 nm.

Bathorhodopsin has an absorption maximum at 2.30 eV (540 nm) and an oscillator strength of approximately 0.9. Assuming that bathorhodopsin contains an all trans PSB retinal chromophore ($\theta_{11,12} = 180°$), the INDO-CISD calculations on the isolated PSB predict a ΔE_{max} at 2.19 eV (566 nm) and an oscillator strength of 1.1. The fact that we have overestimated the oscillator strength of bathorhodopsin suggests that the chromophore in this intermediate is possibly strained leading to torsional distortion which will shift intensity into higher energy transitions.[21] We return to this point later on in this paper where we suggest that compression of the lysine residue during cis-trans isomerization distorts the chromophore in bathorhodopsin. This possibility is supported by the resonance Raman spectra of bathorhodopsin, which suggest a distorted chromophore.[4,15,17]

Potential Surfaces for Isomerization of the Isolated Chromophore. Although the INDO-CISD formalism provides relatively accurate predictions of transition energies, the parametrization is not expected to be as accurate as standard INDO theory for the calculation of absolute barriers to isomerization.[39] Accordingly, we used standard INDO parametrization[49] to calculate the ground-state potential surface, although single and double excitation CI (~130 singles, ~410 doubles) was included to improve the treatment of electron correlation. The repulsion associated with methyl groups was included in an approximate fashion by treating the C_9 and C_{13} methyl groups as point masses separated by 1.52 Å from the corresponding C_9 and C_{13} carbons. The same standard geometry for the rest of the polyene chain was used (see above). Accordingly, the calculated potential surface is not adiabatic and the calculated barrier to ground-state isomerization is likely to be overestimated (see Figure 4). Although there are no activation-energy data on protonated Schiff bases, the thermal isomerization of 11-*cis*-retinal has been studied by Hubbard, who observed activation energies in the range 22.4-26.2 kcal/mol.[50] Since the barrier for 11-cis to 11-trans isomerization in the protonated Schiff base is predicted to be smaller than the corresponding barrier in retinal,[8] we are confident that we are, in fact, overestimating this barrier. Our calculated barrier is slightly larger than that predicted by Salem and Bruckmann using an ab initio formalism (27.2 kcal/mol).[36]

The calculated potential surfaces in the lowest two excited singlet states are shown in Figure 4 and are obtained by adding the INDO-CISD transition energies to the corresponding ground-state relative energies. Note that identical geometries were used in both sets of calculations for a given dihedral angle. Accordingly, the excited-state surfaces are also not adiabatic and will tend to overestimate the barriers to isomerization in both excited states. Our prediction that the first excited singlet state has a negative barrier to isomerization is extremely important to the entire thrust of this paper. It is responsible for the prediction of rapid isomerization times and corresponds to experimental observation.[7]

Origin of the Barrierless $S_1(\pi\pi^*)$ Potential Surface. The lowest lying $\pi\pi^*$ singlet state is the only excited state of the nine excited states investigated which displays a negative barrier for 11-cis to 11-trans isomerization. The origin of this unique behavior can be traced to the interaction of the lowest lying "$^1B_u{}^{*+}$" ionic state and the second excited "$^1A_g{}^{*-}$" state during isomerization. As previously noted, the "$^1A_g{}^{*-}$" state has considerable doubly excited configurational character which provides for a higher degree of correlative stabilization of torsionally orthogonal double-bond states relative to more ionic states which are made up primarily of singly excited configurations.[21,42,44] As shown in Figure 3, the "$^1A_g{}^{*-}$" second excited state starts to drop rapidly in energy relative to the other low-lying states with small changes in $\theta_{11,12}$ from planarity. Mixing of "$^1A_g{}^{*-}$" character into the "$^1B_u{}^{*+}$" state is enhanced by 11,12 torsional distortion, and the repulsion between these two excited state manifolds forces the lowest excited state to drop rapidly in energy. The lowest singlet state, in fact, becomes "$^1A_g{}^{*-}$"-like in character near $\theta_{11,12} = 90°$, producing a steep potential well (see Figure 4). We will subsequently demonstrate that this potential well is responsible for trapping an activated complex which rapidly oscillates between species which will internally convert back to the ground state to produce both 11-cis and 11-trans conformations. The first excited state potential surface is therefore optimal for the rapid and efficient photochemical isomerization of the 11-cis protonated Schiff base.

III. Molecular Dynamics of Cis-Trans Isomerization Rhodopsin

A previous trajectory analysis of cis-trans isomerization in rhodopsin by Warshel predicted that a concerted, "bicycle-pedal" pathway could accomplish an 11-cis (rhodopsin) to 11-trans (bathorhodopsin) conversion in 0.2 ps.[10] The extremely rapid isomerization time is due to the small moment of inertia of the "bicycle-pedal" motion.[10] Unfortunately, the proposed multibond isomerization pathway predicted a photostationary equilibrium sequence of isorhodopsin (9-cis) ⇆ rhodopsin (11-cis) ⇆ bathorhodopsin (all-trans), which is contrary to observation (see above).[12,18,19] Accordingly, a concerted multibond isomerization mechanism appears to be ruled out. We now demonstrate that a direct one-bond 11-cis to 11-trans isomerization in the active site of rhodopsin can take place in approximately 2 ps. Although this isomerization time is an order of magnitude longer than that predicted for the bicycle-pedal model, it is well within the 6-ps upper limit experimentally observed.

Our model of the photochemical transformation of rhodopsin to bathorhodopsin is based on the following assumptions:

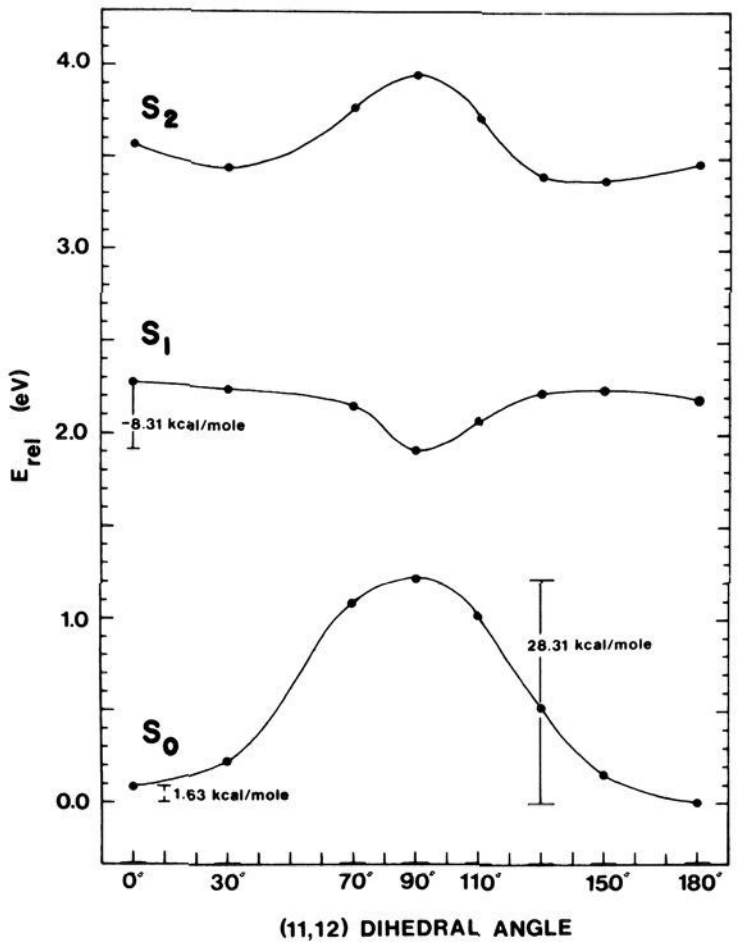

Figure 4. INDO–CISD potential energy surfaces for isomerization about the C_{11}–C_{12} bond in the protonated Schiff base of retinal. The ground-state surface was calculated using standard INDO parametrization and the CI basis set included ~130 single and ~410 double excitations (see text). The excited-state surfaces were obtained by adding the corresponding transition energies (Figure 3) to the ground-state absolute energies. The energies are plotted on a relative scale with the all-trans ($\theta_{11,12} = 180°$) conformation arbitrarily set at $E_{rel} = 0.0$.

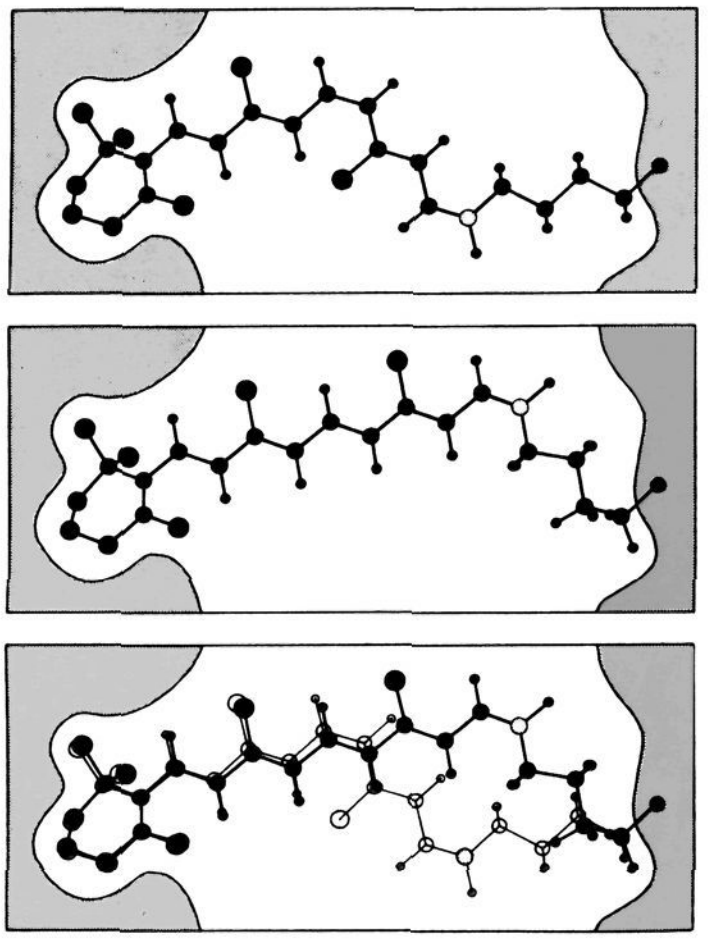

Figure 5. A hypothetical model of the active site of rhodopsin. The top figure shows the conformation of the chromophore and the hydrocarbon residue to lysine in rhodopsin. The middle figure shows the conformation of the chromophore–lysine system in bathorhodopsin. The bottom figure is a superposition of the above two figures to demonstrate the net molecular motion associated with our model of the rhodopsin–bathorhodopsin transformation. The Schiff base nitrogen is indicated with a shaded circle and the hydrogens on the methyl groups are not shown. Note that the lysine residue in bathorhodopsin is deformed out of the plane, and that the cis–trans isomerization is accomplished without significantly disturbing the β-ionylidene ring.

(1) The retinal chromophore is covalently bound to the opsin active site via a protonated Schiff base linkage to a lysine residue of the protein.[3,51-53]

(2) The β-ionylidene ring is trapped in a hydrophobic cleft. During the isomerization, no atom of the β-ionylidene ring is allowed to move by more than 0.05 Å and the center of mass must remain fixed. These assumptions are supported by binding experiments.[54,55]

(3) The photochemical isomerization from the 11-cis to 11-trans conformation is accomplished entirely as a one-bond rotation about the 11,12 bond. All other internal degrees of freedom of the chromophore are fixed at the orginal conformation of the chromophore [11-cis, 6-s-cis (45), 12-s-trans].[56-58]

(4) The first four carbon atoms of the hydrocarbon portion of the lysine residue, and the hydrogens that are bonded to these carbon atoms, are allowed to seek their minimal energy conformation during the isomerization process.[59] No other distortions of the protein are allowed.

Our simplified model for the photochemical transformation of rhodopsin to bathorhodopsin is schematically shown in Figure 5. Although the center of mass of the chromophore–lysine system differs by only 0.86 Å between rhodospin and bathorhodopsin, the moment of inertia associated with the isomerization is relatively large, significantly larger than that associated with Warshel's concerted "bicycle-pedal" model.[10] Nevertheless, the trajectory calculations predict that the transformation from rhodopsin to bathorhodopsin proceeds in approximately 2 ps.

Three sets of trajectory calculations were carried out which differ in the choice of ground and excited state potential surfaces. The first set of trajectories utilizes the potential surfaces shown in Figure 4. Accordingly, the calculations assume the potential surfaces of an isolated chromophore. We will refer to this approximation as model A. The second set of calculations differs only in that the conformational energy associated with the compression and distortion of the lysine residue is included in the ground and excited state potential surfaces.[59] The resulting surfaces are shown in Figure 6 and indicate that conformational distortion of the lysine hydrocarbon chain introduces significant changes in the chromophore–lysine potential surfaces in the 120–180° region of the 11,12 dihedral angle. A new minimum in the ground state potential surface appears at $\theta_{11,12} = 152°$ suggesting that the chromophore in bathorhodopsin is distorted. However, since we are neglecting other degrees of freedom in the chromophore, all of the dis-

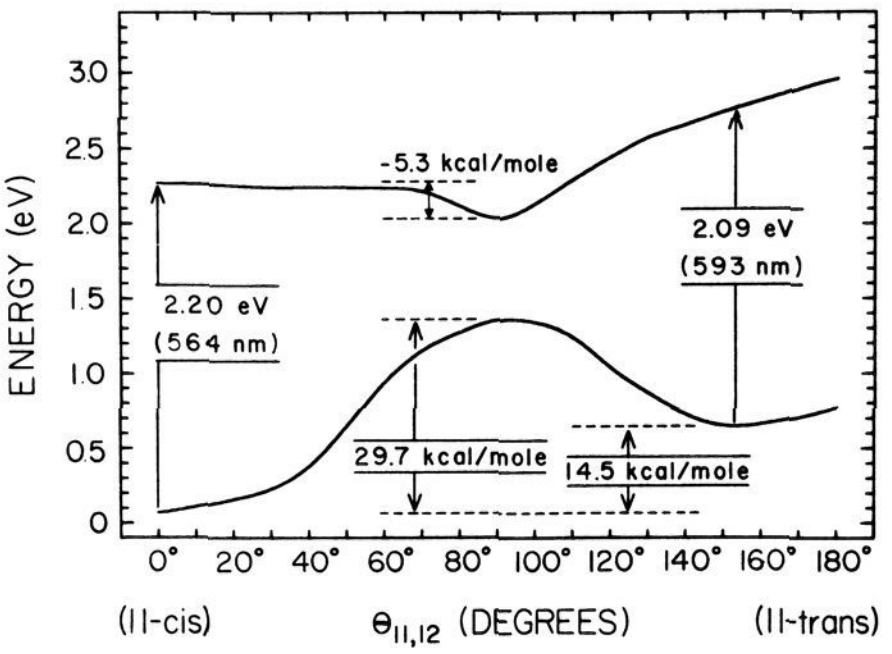

Figure 6. The effect of the conformational distortion of the hydrocarbon residue of lysine on the ground state and first excited $\pi\pi^*$ singlet state potential surfaces of Figure 4. The above potential surfaces represent model B.

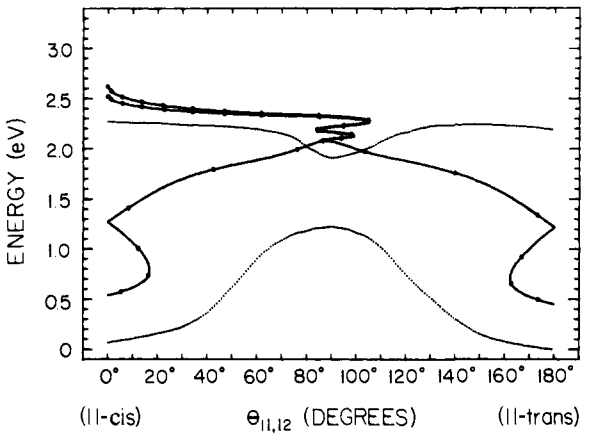

Figure 7. Molecular dynamics of cis-trans isomerization in rhodopsin based on the potential surfaces of Figure 4 (model A). The molecule reaches the activated complex in ~0.8 ps and oscillates in the activated complex with an average frequency for dihedral torsion of $\sim 3.4 \times 10^{12}$ Hz (110 cm^{-1}). The lower left trajectory leads to the starting geometry (rhodopsin) in 1.9 ps; the lower right trajectory leads to isomerized product (bathorhodopsin) in 2.0 ps. These trajectories are shown in boldface in Table I, and along with those which precede them, are responsible for depleting the $S_1(\pi\pi^*)$ surface leaving a fraction of less than e^{-1} (0.37) of the molecules in the excited state. The solid circles indicate trajectory increments of 0.1 ps.

tortion is localized in the 11,12 dihedral coordinate, which is not realistic. INDO-CISD ground state conformational energy minimization suggests that the distortion in the chromophore would be displaced into the C_7-C_{10} and C_{12}-C_{15} regions of the chromophore. However, the potential surfaces shown in Figure 6 (hereafter referred to as model B) are adequate for determining the qualitative effect that the lysine residue will have on the quantum yield and trajectory times for cis-trans isomerization. The third model (C) includes the effects that a counterion has on the potential surfaces. Although the counterion has a dramatic effect on the ground-state potential surface, it has a minor effect on the excited-state surface. Models B and C yield almost identical trajectories and we will therefore limit our preliminary discussion to a comparison of models A and B. Model C, which is more speculative, will be discussed in detail in a separate section.

The semiempirical molecular dynamic procedures used for the present investigation of isomerization trajectories are based on the semiclassical formalisms of ref 60 and 61. Detailed discussions of our procedures are presented in ref 62 and 63, where they are compared to the more exact semiclassical treatments which explicitly include vibrational force fields. It is sufficient to note for the purposes of the present discussion that we have adopted parametrization which will overestimate trajectory times.

The formalism places restraints on the energy available to the torsional motion by limiting the source of the torsional kinetic energy to that which is provided by the potential surface. Accordingly, excess vibrational energy is prevented from partitioning into the torsional kinetic energy. In contrast, an efficient pathway is provided for transfer of torsional kinetic energy into "nonproductive" vibrational modes based on a vibrational continuum approximation given by

$$(\Delta E_{kin}/\Delta t)_{t=\tau} = -C_m E_{kin}^2(\tau) \quad (\Delta E_{kin} > h\nu_1) \qquad (1)$$

where $(\Delta E_{kin}/\Delta t)_{t=\tau}$ is the rate of loss of torsional kinetic energy at trajectory time τ, $E_{kin}(\tau)$ is the torsional kinetic energy at $t = \tau$, and $h\nu_1$ is the energy of the lowest vibrational mode capable of scavenging torsional kinetic energy (see below). C_m is a semiempirical constant which is equal to the vibrational coupling efficiency. An approximate upper limit to C_m can be obtained by assuming that a single vibrational quantum transition is present in the molecule which is exactly equal in energy to the instantaneous torsional kinetic energy and that this vibrational mode can scavenge all of the torsional kinetic energy at a rate equal to the frequency of the vibration. This assumption yields an upper limit of

$$C_m \lesssim 1/h \qquad (2)$$

where h is Planck's constant. Molecular dynamics calculations including explicit vibrational force fields have been used to calibrate C_m. Equation 2, in conjunction with eq 1, is found to overestimate the magnitude of vibrational scavenging by factors of 2-10.[62,63] However, the continuum model embodied in eq 1 will invariably overestimate coupling when the torsional kinetic energy is lower than the energy of the lowest mode available for vibrational scavenging. Accordingly, $(\Delta E_{kin}/\Delta t)$ is set equal to zero whenever E_{kin} is less than the energy of this lowest mode.

The trajectory calculations presented here are designed to overestimate the trajectory times. Accordingly, we have chosen a relatively large value for C_m of $\frac{1}{2}h^{-1}$ and a relatively small $h\nu_1$ of 50 cm^{-1}.[64] We are confident that these parameters will overestimate vibrational scavenging of the torsional kinetic energy. Furthermore, the possibility of reverse coupling whereby vibrational energy is transferred back into the torsional degree of freedom is ignored in our trajectory calculation. The above approach virtually guarantees that our trajectories will overestimate isomerization time, probably by a factor of 1.4 or more.

The experimental observation of a wavelength-independent quantum yield for rhodopsin isomerization indicates that excess vibrational energy of the chromophore (E_{vib}) is rapidly transferred to the protein matrix. We simulate this process using a density of states approximation:[62,63]

$$(\Delta E_{vib}/\Delta t)_{t=\tau} = -|\Delta E_{vib}/\Delta t|_{av}\{1 - e^{-\rho[E_{vib}(\tau)-kT]}\} - (\Delta E_{kin}/\Delta t)_{t=\tau} \qquad (3)$$

where $(\Delta E_{vib}/\Delta t)_{t=\tau}$ is the rate of vibrational relaxation at trajectory time τ, $|\Delta E_{vib}/\Delta t|_{av}$ is the absolute (exponential) average vibrational relaxation rate, ρ is the density of states factor, $E_{vib}(\tau)$ is the vibrational energy at trajectory time τ, k is the Boltzmann constant, T is the temperature (300 K), and $(\Delta E_{kin}/\Delta t)_{t=\tau}$ is calculated using eq 1. Equation 3 indicates that vibrational energy is lost through relaxation processes but gained through transfer of torsional kinetic energy into the vibrational manifold. The salient parameters were adjusted to produce a wavelength-independent quantum yield for isomerization yielding $|\Delta E_{vib}/\Delta t|_{av}$ = 2 eV/ps and ρ = 1 eV^{-1} (see below).

Isomerization trajectories based on models A and B are shown in Figures 7 and 8. The molecules are promoted into the excited state from a rest position with a resulting excess vibrational energy (E_{vib}) of 0.25 or 0.35 eV. This vibrational energy is rapidly dissipated (eq 3), and the resultant trajectories enter the activated complex with almost identical vibrational energy. The rapid vibrational relaxation, and the fact that vibrational energy is prevented from partitioning into torsional kinetic energy, produces isomerization kinetics essentially independent of excitation energy in agreement with experiment.[2,5,7] The trajectories based on model A (Figure 7) predict an excited-state lifetime of ~1.4 ps, a quantum yield for isomerization of 0.57, and an intrinsic isomerization time to form the relaxed ground state of ~2.0 ps.[65] The trajectories based on model B (Figure 8) predict an excited-state lifetime of ~1.5 ps, a quantum yield of isomerization of 0.61, and an intrinsic isomerization time to form the relaxed ground state of ~2.3 ps.[65] The fact that we are underestimating the quantum yields for isomerization suggests that we are overestimating the isomerization times, an observation discussed in

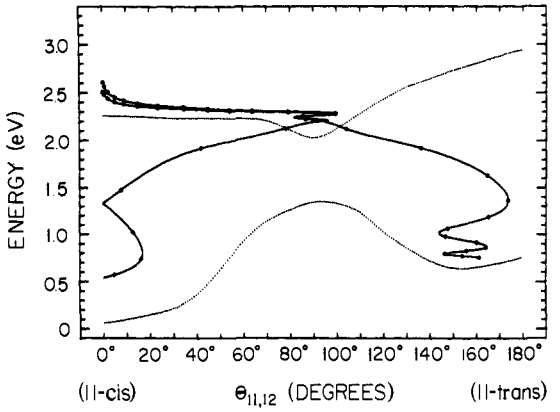

Figure 8. Molecular dynamics of cis-trans isomerization in rhodopsin based on the potential surfaces of Figure 6 (model B). The molecule reaches the activated complex in ~1.1 ps and oscillates with a frequency of torsional motion of $\sim 3.9 \times 10^{12}$ Hz (130 cm^{-1}). The lower left trajectory leads to the starting geometry (rhodopsin) in 2.1 ps; the lower right trajectory leads to distorted transoid ($\theta_{11,12} = 152°$) product (bathorhodopsin) in 2.3 ps. These trajectories are shown in boldface in Table II, and along with those which precede them, are responsible for depleting the $S_1(\pi\pi^*)$ surface leaving a fraction of less than e^{-1} (0.37) of the molecules in the excited state. The solid circles indicate trajectory increments of 0.1 ps.

greater detail below. Nevertheless, the calculated isomerization times are well within the ambient temperature experimental upper limit of 6 ps.[11]

Both sets of trajectories predict that the excited-state species is trapped in an activated complex which has a lifetime of approximately 0.5 ps. This activated complex rapidly oscillates between two components which preferentially decay to form isomerized product (bathorhodopsin) or the original starting material (rhodopsin). The nature of this activated complex supports the common excited state hypothesis outlined in ref 7 and virtually guarantees a quantum yield greater than 0.5 as discussed below.

Calculation of the Quantum Yield of Cis-Trans Photoisomerization. Our model of the photochemical conversion of rhodopsin to bathorhodopsin should be capable of accounting for both the rapid (<6 ps) formation time and the relatively high quantum yield (ϕ) of 0.67 measured for this process.[66] A theoretical prediction of ϕ based on our trajectory analysis can be obtained by calculating the probability of crossing into the ground state $a_0^2(\tau)$, as a function of trajectory time, τ. A time-dependent quantum mechanical treatment yields[10,60,61]

$$a_0^2(\tau) = \left\{ \int_0^\tau \left[\left\langle \psi_0 \left| \frac{\partial \psi_1}{\partial t} \right\rangle a_1(t) \times \exp\left\{ -\frac{i}{\hbar} \int_0^t \Delta E_{10} dt' \right\} \right] dt \right\}^2 \quad (4)$$

where ψ_0 and ψ_1 are the electronic wave functions of the ground and excited state and ΔE_{10} ($=E_1 - E_0$) is the time-dependent potential energy difference between the excited state and the ground state. Unfortunately, solution of the nonadiabatic coupling function $\langle \psi_2 | \partial \psi_1 / \partial t \rangle$ is not possible within the confines of our semiempirical trajectory formalism without the introduction of serious ad hoc assumptions. Accordingly, we will calculate $a_0^2(\tau)$ using a semiclassical solution based on the treatments of Stuckelberg[65] and Miller and George[61] (see ref 62 for derivation):

$$a_0^2(\tau) = \exp - \left\{ \left(\frac{4\Delta W(\tau)}{3\hbar} \right) \left[\frac{2\Delta W(\tau)}{(\partial^2 \Delta E_{10}/\partial t^2)_{t=\tau}} \right]^{1/2} \right\} \quad (5)$$

where $\Delta W(\tau)$ is the adiabatic potential energy difference between the ground and excited state adjusted with respect to the

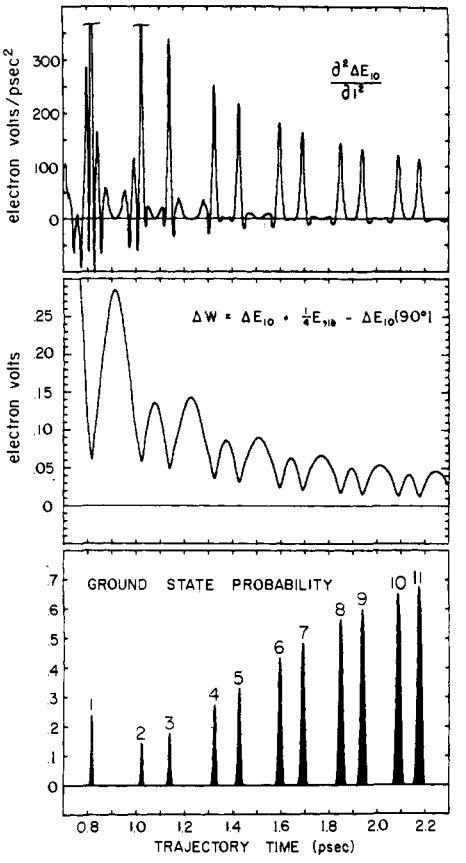

Figure 9. An analysis of the probability that an individual trajectory will cross into the ground state as a function of trajectory time for model A (Figure 7 and Table I). The calculation is based on eq 6 and the salient time-dependent variables are plotted in the top two graphs.

Born-Oppenheimer local minimum:[62,63]

$$\Delta W(\tau) = \Delta E_{10}(\tau) - \Delta E_{10}(\text{lm}) + \tfrac{1}{4}E_{\text{vib}}(\tau) \quad (6)$$

ΔE_{10}(lm) is the difference in the excited-state and ground-state potential energy surfaces at their minimum energy separation and occurs in the present study at a 11,12 dihedral angle of 90°.

We will confine our initial discussion to the trajectories calculated for model A (Figure 7). A comparison of models A and B will then be presented to demonstrate a possible mechanism by which the protein can influence the dynamics of the isomerization process to improve the quantum yield of isomerization. The techniques used to determine the quantum yield are identical for both models.

As shown in Figure 9, the ground-state probability [$a_0^2(\tau)$] passes through a series of sharply peaked maxima as a function of time as the trajectory passes through the 90° dihedral angle on the potential surface (Figure 7). The first pass through the 90° region occurs at 0.816 ps and has a probability of transferring into the ground state of 0.237. Accordingly, ~24% of the molecules in the excited state internally convert to the ground state and yield isomerized (11-trans) product in ~1.4 ps. (The ground-state probability is larger on the first pass, relative to the second and third passes, because of the large torsional velocity which is present upon the first passage into the activated complex.) The second pass through the 90° region occurs at 1.029 ps with a ground-state probability of 0.143 transferring ~11% of the remaining excited-state species to the ground state. However, the subsequent ground-state trajectory yields the original 11-cis conformation in ~1.6 ps. If we continue to split the trajectory into ground- and excited-state pathways we obtain the results given in Table I. After ten passes through the 90° region, >99% of the molecules are in

Table I. Statistical Analysis of the Quantum Yield for Cis-Trans Isomerization Based on Probabilities of Trajectory Splitting into the Ground State (Model A)

pass no.[a]	τ, ps[b]	$a_0^2(\tau)$[c]	% S_1[d]	% S_0^{cis}[e]	% S_0^{trans}[f]	τ_0*[g]	τ_0^r[h]
1	0.816	0.237	76.3		23.7	1.101 (t)	1.396
2	1.029	0.143	65.4	10.9	23.7	1.318 (c)	1.616
3	1.138	0.176	53.9	10.9	35.2 (11.5)	1.425 (t)	1.738
4[i]	**1.324**	**0.275**	**39.1**	**25.7 (14.8)**	**35.2**	**1.630 (c)**	**1.928**
5[i]	**1.427**	**0.331**	**26.2**	**25.7**	**48.1 (12.9)**	**1.722 (t)**	**2.035**
6	1.595	0.434	14.8	3.71 (11.4)	48.1	1.910 (c)	2.208
7	1.691	0.484	7.6	37.1	55.3 (7.2)	1.992 (t)	2.305
8	1.849	0.564	3.3	41.4 (4.3)	55.3	nc[j]	nc[j]
9	1.940	0.599	1.3	41.4	57.3 (2.0)	nc	nc
10	2.088	0.652	0.5	42.2 (0.8)	57.3	nc	nc

[a] Trajectory pass through the 90° dihedral angle of the 11,12 bond. [b] Trajectory time. [c] Probability of crossing into the ground state at τ. [d] Percent of molecules remaining in the excited state after trajectory splitting. [e] Percent of molecules which will equilibrate to form unisomerized (11-cis) conformation (Δ % for individual trajectory in parentheses). [f] Percent of molecules which will equilibrate to form isomerized (11-trans) conformation (Δ % for individual trajectory in parentheses). [g] Total trajectory time (ps) until molecule is in a planar configuration with excess vibrational energy. The resulting geometry is indicated in parentheses (t = 11-trans, c = 11-cis). [h] Total trajectory time (ps) for molecule to reach "relaxed" ground state (see text). [i] Trajectories listed in boldface are shown in Figure 7. [j] nc = not calculated.

Table II. Statistical Analysis of the Quantum Yield for Cis-Trans Isomerization Based on Probabilities of Trajectory Splitting into the Ground State (Model B)

pass no.[a]	τ, ps[b]	$a_0^2(\tau)$[c]	% S_1[d]	% S_0^{cis}[e]	% S_0^{trans}[f]	τ_0*[g]	τ_0^r[h]
1	1.142	0.308	69.2		30.8	1.506 (t)	2.004
2	1.271	0.202	55.2	14.0	30.8	1.552 (c)	1.849
3[i]	**1.423**	**0.190**	**44.7**	**14.0**	**41.3 (10.5)**	**1.787** (t)	**2.285**
4[i]	**1.537**	**0.232**	**34.3**	**24.4 (10.4)**	**41.3**	**1.828** (c)	**2.124**
5	1.679	0.282	24.6	24.4	51.0 (9.7)	2.070 (t)	2.554
6	1.787	0.340	16.2	32.8 (8.4)	51.0	2.084 (c)	2.381
7	1.927	0.400	9.7	32.8	57.5 (6.5)	2.305 (t)	2.813
8	2.030	0.455	5.3	37.2 (4.4)	57.5	2.332 (c)	2.629
9	2.169	0.507	2.6	37.2	60.2 (2.7)	nc[j]	nc[j]
10	2.269	0.550	1.2	38.6 (1.4)	60.2	nc	nc
11	2.407	0.590	0.5	38.6	60.9 (0.7)	nc	nc
12	2.506	0.620	0.2	38.9 (0.3)	60.9	nc	nc

[a-f] See Table I. [g] Total trajectory time (ps) until molecule reaches "edge" of its ground-state trajectory with excess vibrational energy. The resulting geometry is indicated in parentheses (t = 11-transoid, c = 11-cis). [h] Total trajectory time (ps) for molecule to reach "relaxed" ground state (see text). [i] Trajectories listed in boldface are shown in Figure 8. [j] nc = not calculated.

the ground state [57% are in the (isomerized) 11-trans configuration, 42% are in the (unisomerized) 11-cis configuration]. Accordingly, the quantum yield for cis-trans isomerization based on model A is 0.57. This theoretical value is in reasonably good agreement with the observed quantum yield for bleaching of rhodopsin of 0.67.[66]

We should note that the theoretical value would increase if both the "speed" of the torsional motion and the rate of radiationless decay were increased. Since both of these values could be increased by adjusting the semiempirical parameters, it would be possible to force our model to exactly predict the quantum yield. As noted in the previous section, however, we have chosen conservative values for these parameters so as to overestimate the isomerization time. Accordingly, the fact that we are underestimating the quantum yield is in keeping with our objective and suggests that we are, in fact, overestimating the time required for forming bathorhodopsin from rhodopsin.

An identical analysis with that described above can be used to determine the quantum yield for isomerization based on model B (see Figure 8). The results are shown in Table II and yield a value of $\phi = 0.61$. The improvement in the calculated quantum yield is due entirely to the perturbation that the lysine residue introduces into the potential surfaces in the ground and excited state (Figure 6).

Potential Effect of Counterions on Isomerization Dynamics. The trajectory calculations discussed above were carried out for a protonated Schiff base completely isolated from counterions or negatively charged groups. There is experimental evidence to suggest, however, that one or more counterions are likely to be in close proximity to the chromophore.[5,10] Furthermore, the deuterium isotope effect observed by Peters et al.[13] suggests that at low temperature the rate-limiting step may involve a hydrogen transfer to, or from, a local negative counterion. At ambient temperature, however, we believe that the isomerization of the chromophore is the rate-limiting step. A more detailed discussion of this problem, which is consistent with our trajectory calculations, may be found in ref 5.

Honig and co-workers have suggested that a negative counterion (a carboxylate anion of aspartic or glutamic acid) may be located at an ionic bond length of approximately 3 Å from the Schiff-base nitrogen.[5,8,9] Our INDO-CISD calculations predict that a carboxylate anion located such that one of the oxygen atoms is positioned equidistant (3 Å) from both the imino nitrogen and the C_{15} carbon (Figure 10) will blue shift the calculated transition energy of the rhodopsin chromophore by 0.41 eV (Figure 11).[68] Accordingly, the calculated transition energy will increase from 2.20 (564 nm) to 2.61 eV (475 nm), which is in slightly better agreement with the observed λ_{max} absorption of 497 nm. The large blue shift is associated with the preferential stabilization of the ground state relative to the excited state due to migration of 0.335 units of charge out of the C_{15}=N_{16} moiety upon excitation into the first excited singlet state (see Figure 1 noting that the combined charge on C_{15} and N_{16} is +0.158 in the ground state but −0.177 in the Franck-Condon excited state).[68] The motion of the chromophore during the early stages of the isomerization slightly increases electrostatic stabilization of the excited state

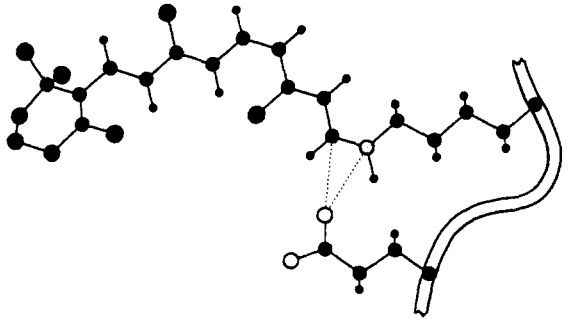

Figure 10. A hypothetical model of the active site of rhodopsin including a counterion consisting of the carboxylate group of a glutamic acid residue. One of the oxygen atoms of the carboxylate group is placed 3 Å (dotted lines) from both the C_{15} carbon and the N_{16} imino nitrogen (shaded circle) atoms. The two oxygen atoms (open circles) of the carboxylate group are each assigned a charge of −0.5, the carboxylate carbon is assigned a charge of +0.2, and the carbon bonded to the above is assigned a charge of −0.2. The remaining atoms of the glutamic acid residue were not included in the calculation of intermolecular nonbonded interactions. A standard geometry for the carboxylate group was assumed: $R_{C=O}$ = 1.3 Å, R_{C-C} = 1.52 Å, ∠OCO = 120°. The ribbon connecting the lysine and glutamic acid residues is included to schematically indicate that both residues are attached to the same protein backbone; it is not intended to accurately portray the geometry of the backbone.

which, in turn, generates a slightly more negative barrier to isomerization (Figure 11). The effect is relatively small, however, and the isomerization trajectories are almost identical with those calculated for model B which included only the effect associated with the compression of the lysine residue.

We should also mention, however, that a counterion placed in the region of the C_{10}-C_{11} atoms would have exactly the opposite effect to that described above. The excited state would be more stabilized than the ground state, isomerization time would increase, and the quantum yield for isomerization would decrease. Accordingly, the location of the counterion(s) is crucial to the ultimate dynamics of the rhodopsin to bathorhodopsin transformation.

IV. Molecular Dynamics of Isomerization in Solution

Huppert, Rentzepis, and Kliger investigated the isomerization kinetics of 11-*cis*-retinyl PSB compounds in solution and observed nanosecond cis-trans isomerization times.[69] At first glance one might assume that this observation precludes the possibility of picosecond isomerization times in the visual pigment. However, there are two important differences between a solution environment and the hydrophobic opsin protein environment that would generate significantly different isomerization kinetics.

(1) The counterion in solution is very tightly bound and will significantly restrict the motion of the C_{12}-N_{16} moiety during isomerization. Any motion of the counterion will disturb a large solvent shell which is many solvent molecules thick due to the strength of the reaction field. These considerations suggest that the β-ionylidene ring, which is also very large, will have to move a few angstroms during the isomerization. The effective moment of inertia for isomerization in solution is therefore significantly larger than that of the molecular motion depicted in Figure 5. We estimate that these effects would increase isomerization time by factors of 5-50, a large effect but not in itself sufficient to account for the three orders of magnitude kinetic difference between protein and solution environments.

(2) A more important effect is associated with the free energy of solvation which will significantly alter the ground- and excited-state potential surfaces. Waddell and Hopkins have investigated the effect of excitation wavelength and solvent environment on the isomer distribution of retinals at photoequilibrium.[70] These investigators observed significant

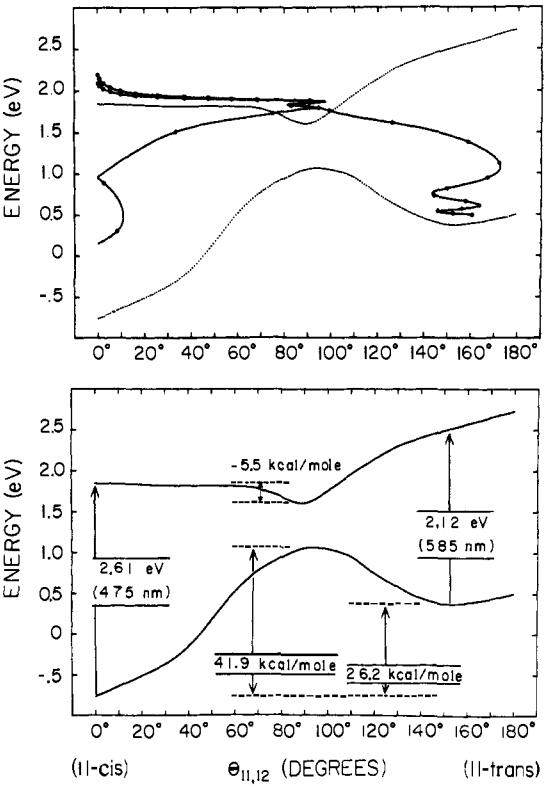

Figure 11. The effect of the counterion described in Figure 10 on the ground state and first excited $\pi\pi^*$ singlet state potential surfaces of Figure 6. The above potential surfaces include the contributions of both the counterion and the conformational distortion of the lysine residue. The counterion lowers the energy of the 11-cis ($\theta = 0°$) ground state by 30.7 kcal/mol and lowers the energy of the 11-cis first excited singlet state by 21.3 kcal/mol. The counterion has only a minor effect on the excited-state potential surface which results in isomerization trajectories very similar to those calculated for model B (Figure 8). The figure at the top shows two trajectories which correspond to those described in Figure 8.

solvent effects on photoisomerization products which indicate that the formation of cis isomers is favored in polar (alcoholic) solvent. Although similar investigations have not been performed on the protonated Schiff base of retinal, the evidence suggests that polar solvents will decrease the quantum yield of cis-trans isomerization by increasing the barrier for this process in the excited state. Accordingly, it is very likely that the barrier for cis-trans isomerization of the protonated Schiff base in polar solvent is no longer negative. The presence of even a small barrier to isomerization would increase the kinetics by one to three orders of magnitude relative to a barrierless process. Radiationless and radiative processes into the ground state would then compete favorably with isomerization, thereby lowering the quantum yield of isomerization. The nanosecond isomerization times observed by Huppert et al. in methanol solvent are consistent with this interpretation.[69]

V. Comments and Conclusions

(1) INDO-CISD molecular orbital theory predicts that cis-trans isomerization in the isolated protonated Schiff base of retinal is a barrierless process in the excited state which can proceed in ~2 ps with a high quantum efficiency of ~0.6.

(2) A hypothetical model of the active site of rhodopsin suggests that conformational distortion of the lysine residue will slightly increase the barrier to isomerization, but the barrier is still negative in the excited state. Although individual excited-state trajectories are slowed down by ~40% when the free energy of compression of the lysine residue is included, probabilities of intercepting the ground state are enhanced by ~30%, which results in the same approximate conversion times of ~2 ps.

(3) The inclusion of a counterion in the vicinity of the $C_{15}=N_{16}$ group increases the isomerization barrier in the ground state but slightly decreases an already negative barrier in the excited state. Accordingly, a counterion can decrease the probability of a thermal isomerization of the visual pigment. The location of the counterion is critical and a counterion placed at locations other than the one proposed in this paper could significantly increase or decrease the calculated photochemical isomerization time.

(4) The conformational distortion of the lysine residue is predicted to distort the chromophore in bathorhodopsin, preventing it from reaching a planar all-trans conformation. INDO-CISD calculations suggest that the distortion will be concentrated in the C_7-C_{10} and/or C_{12}-C_{15} regions of the chromophore.

(5) The ground-state barrier to thermal cis-trans isomerization in rhodopsin is predicted to be in the range 29.7-41.9 kcal/mol. Bathorhodopsin is predicted to have a free energy 14.5-26.2 kcal/mol higher than rhodopsin. The lower values include the effect of lysine conformational distortion and the inherent electronic properties of the chromophore. The larger values additionally include the effect of a counterion on the potential surfaces. The experimental values lie somewhere in between.[4,7]

(6) The bathochromic shift of the absorption maximum of bathorhodopsin relative to rhodopsin is attributed to the effects of a counterion as well as the conformational distortion of the chromophore due to compression of the lysine residue in bathorhodopsin. Our calculations predict bathochromic shifts in the range of 29-110 nm. The experimental value of 43 nm indicates that our single counterion model overestimates the shift and suggests that two counterions may be present in the active site of rhodopsin.

(7) We conclude that the classical concept that bathorhodopsin is formed by a cis-trans isomerization is the most realistic model for the first step in the rhodopsin bleaching cycle.

Acknowledgments. This work was supported in part by grants from the National Institutes of Health, the donors of the Petroleum Research Fund, administered by the American Chemical Society, Research Corporation, and the National Center for Atmospheric Research. The authors are grateful to J. A. Bennett, B. M. Pierce, and Professors B. Honig, D. Kliger, J. Lugtenberg, R. Mathies, and A. Warshel for interesting and helpful discussions.

References and Notes

(1) UCAR Graduate Student Fellow.
(2) Honig, B. *Annu. Rev. Phys. Chem.* **1978,** *29*, 31, 57.
(3) Eyring, G.; Mathies, R. *Proc. Natl. Acad. Sci. U.S.A.* **1979,** *76*, 33.
(4) Doukas, A. G.; Aton, B.; Callender, R. H.; Ebrey, T. G. *Biochemistry* **1978,** *17*, 2430.
(5) Honig, B.; Ebrey, T.; Callender, R. H.; Dinur, U.; Ottolenghi, M. *Proc. Natl. Acad. Sci. U.S.A.* **1979,** *76*, 2503.
(6) Green, B.; Monger, T.; Alfano, R. ; Aton, B.; Callender, R. *Nature (London)* **1977,** *264*, 179.
(7) Rosenfeld, T.; Honig, B.; Ottolenghi, M.; Hurley, J.; Ebrey, T. G. *Pure Appl. Chem.* **1977,** *49*, 341.
(8) Honig, B.; Greenberg, A.; Dinur, U.; Ebrey, T. G. *Biochemistry* **1976,** *15*, 4593.
(9) Honig, B.; Ebrey, T. *Biophys. J.* **1976,** *16*, 98a.
(10) Warshel, A. *Nature (London)* **1976,** *260*, 679.
(11) Busch, G.; Applebury, M.; Lamola, A.; Rentzepis, P. *Proc. Natl. Acad. Sci. U.S.A.* **1972,** *69*, 2802.
(12) Applebury, M. L.; Peters, K.; Rentzepis, P. *Biophys. J.* **1978,** *23*, 375, 382.
(13) Peters, K.; Applebury, M.; Rentzepis, R. *Proc. Natl. Acad. Sci. U.S.A.* **1977,** *74*, 3119.
(14) van der Meer, K.; Mulder, J. J. C.; Lugtenberg, J. *Photochem. Photobiol.* **1976,** *24*, 363.
(15) Lewis, A. *Proc. Natl. Acad. Sci. U.S.A.* **1978,** *75*, 549.
(16) Favrot, J.; Leclercq, J. M.; Roberge, R.; Sandorfy, C.; Vocelle, D. *Photochem. Photobiol.* **1979,** *29*, 99.
(17) Warshel, A. *Proc. Natl. Acad. Sci. U.S.A.* **1978,** *75*, 2558.
(18) Yoshizawa, T.; Wald, G. *Nature (London)* **1963,** *197*, 1279.
(19) Hubbard, R.; Kropf, A. *Proc. Natl. Acad. Sci. U.S.A.* **1958,** *44*, 215.
(20) The dihedral angle is represented by the symbol θ to differentiate it from the quantum yield of isomerization (ϕ).
(21) (a) Birge, R. R.; Schulten, K.; Karplus, M. *Chem. Phys. Lett.* **1975,** *31*, 451. (b) Birge, R. R.; Schulten, K.; Hubbard, L. M.; Karplus, M., to be published.
(22) Birge, R. R.; Bennett, J. A.; Pierce, B. M.; Thomas, T. M. *J. Am. Chem. Soc.* **1978,** *100*, 1533.
(23) Birge, R. R.; Pierce, B. M. *J. Chem. Phys.* **1979,** *70*, 165.
(24) Suzuki, H.; Nakachi, K.; Komatsu, T. *J. Phys. Soc. Jpn.* **1974,** *37*, 177.
(25) Suzuki, H.; Nakachi, K.; Komatsu, T. *J. Phys. Soc. Jpn.* **1974,** *37*, 741.
(26) Kliger, D. S.; Milder, S. J.; Dratz, E. A. *Photochem. Photobiol.* **1977,** *25*, 277.
(27) Wiesenfeld, J. R.; Abrahamson, E. W. *Photochem. Photobiol.* **1968,** *8*, 487.
(28) Suzuki, H.; Takizawa, N.; Komatsu, T. *Prog. Theor. Phys. Suppl.*, **1970,** *246*, 16.
(29) Suzuki, H.; Komatsu, T.; Kato, T. *J. Phys. Soc. Jpn.* **1973,** *34*, 156.
(30) Schaffer, A. M.; Waddell, W. H.; Becker, R. S. *J. Am. Chem. Soc.* **1974,** *96*, 2063.
(31) Schaffer, A. M.; Yamaoka, T.; Becker, R. S. *Photochem. Photobiol.* **1975,** *21*, 297.
(32) Inuzuka, K.; Becker, R. S. *Nature (London)* **1968,** *219*, 383.
(33) Pullman, A.; Pullman, B. *Proc. Natl. Acad. Sci. U.S.A.* **1961,** *47*, 7.
(34) Weimann, L. J.; Maggiora, G. M.; Blatz, P. E. *Int. J. Quantum Chem., Quantum Biol. Symp.* **1975,** *No. 2*, 9.
(35) Warshel, A.; Karplus, M. *J. Am. Chem. Soc.* **1974,** *96*, 5677.
(36) Salem, L.; Bruckmann, P. *Nature (London)* **1975,** *258*, 526.
(37) Salem, L. *Acc. Chem. Res.* **1979,** *12*, 87.
(38) For an excellent discussion of PPP parametrization see: Dewar, M. J. S.; Morita, T. *J. Am. Chem. Soc.* **1969,** *91*, 796.
(39) Hubbard, L. M.; Birge, R. R., to be published.
(40) Del Bene, J.; Jaffe, H. H. *J. Chem. Phys.* **1968,** *48*, 1807, 4050; **1968,** *49*, 1221.
(41) Ellis, R. L.; Kuehnlenz, G.; Jaffe, H. H. *Theor. Chim. Acta* **1972,** *26*, 131.
(42) Sichel, J. M.; Whitehead, M. A. *Theor. Chim. Acta* **1967,** *7*, 32.
(43) Schulten, K.; Karplus, M. *Chem. Phys. Lett.* **1972,** *14*, 305.
(44) Schulten, K.; Ohmine, I.; Karplus, M. *J. Chem. Phys.* **1976,** *64*, 4422.
(45) If m is the number of doubly occupied orbitals and n the number of unoccupied orbitals, the total number of singly excited configurations equals mn. The number of spin-paired doubly excited singlet confiruations is given by $\{[m(m-1)/2] + m\}\{[n(n-1)/2] + n\}$. The number of spin-spin coupled doubly excited singlet configurations is given by $\{[(m-1)(m-2)/2] + m - 1\}\{[(n-1)(n-2)/2] + n - 1\}$.
(46) Birge, R. R.; Bennett, J. A.; Fang, H. L-B.; Leroi, G. E. "Advances in Laser Chemistry," Zewail, A. H., Ed.; Springer Series in Chemical Physics, Vol. III; Springer-Verlag: New York, 1978; pp 347-354.
(47) The ground-state INDO-CISD calculations indicate that the σ electron density and charge on nitrogen changes from 3.47 ($q_N^{\sigma} = +0.53$)(11-cis) to 3.42 ($q_N^{\sigma} = +0.58$)(11,12 orthogonal) as a function of 11,12 dihedral angle. These values suggest that a nitrogen atom core charge of 0.55 (rather than 1.0) represents a more realistic value to use within the PPP approximation. However, the fact that a relatively large change in σ electron distribution occurs during isomerization suggests that restricted π-electron procedures, such as the PPP method, may be incapable of properly describing some of the more subtle electronic features associated with double-bond isomerization.
(48) Irving, C. S.; Leermakers, P. A. *Photochem. Photobiol.* **1968,** *7*, 665. Waddell, W.; Becker, R. S. *J. Am. Chem. Soc.* **1971,** *93*, 3788.
(49) Pople, J. A.; Segal, G. A. *J. Chem. Phys.* **1976,** *44*, 3289.
(50) Hubbard, R. *J. Biol. Chem.* **1966,** *241*, 1814.
(51) Oseroff, A.; Callender, R. *Biochemistry* **1974,** *13*, 4243.
(52) Sulkes, M.; Lewis, A.; Marcus, M. *Biochemistry* **1978,** *17*, 4712-4722.
(53) Aton, B.; Doukas, A.; Narva, D.; Callender, R. H.; Honig, B.; Dinur, U. *Biophys. J.* **1979,** *25*, 76a.
(54) Blatz, P. E.; Lin, M.; Balasvbramanigan, P.; Balasvbramanigan, V.; Bewhurst, P. B. *J. Am. Chem. Soc.* **1969,** *91*, 5930.
(55) Matsumoto, H.; Yoshizawa, T. *Nature (London)* **1974,** *258*, 523.
(56) Birge, R. R.; Sullivan, M. J.; Kohler, B. E. *J. Am. Chem. Soc.* **1976,** *98*, 358.
(57) Burke, D. C.; Faulkner, T. R.; Moscowitz, A. *Exp. Eye Res.* **1973,** *17*, 557.
(58) (a) Callender, R. H.; Doukas, A.; Crouch, R.; Nakanishi, K. *Biochemistry* **1976,** *15*, 1621. (b) Ebrey, T.; Govindjee, R.; Honig, B.; Pollack, E.; Chan, W.; Crouch, S.; Yudd, A.; Nakanishi, K. *Biochemistry* **1975,** *14*, 3933.
(59) (a) The conformational energy of the lysine residue was calculated using the empirical potential functions proposed by Lifson and Warshel.[59b] The parameters for the potential functions were taken from ref 59b (lysine carbons and hydrogens) and 59c (protonated nitrogen atom). The conformation of the lysine residue in rhodopsin was arbitrarily assumed to be that which yielded the minimum force field free energy with no external constraints (see top of Figure 5). The conformation of the lysine residue as a function of 11,12 dihedral angle was determined by force field minimization with the constraint that only the first four carbon atoms, and their associated hydrogens, were allowed to move in response to motion of the polyene moiety. (See, for example, middle diagram of Figure 5 and note that the lysine carbon atoms are counted starting at the polyene end.) The fact that a "no constraint" minimization of the lysine residue was performed for the planar 11-*cis*-retinyl geometry will probably bias the calculation to overestimate the "true" conformational energy of the lysine residue in bathorhodopsin. This bias will also tend to slightly increase the calculated isomerization times. (b) Lifson, S.; Warshel, A. *J. Chem. Phys.* **1968,** *49*, 5116. Warshel, A.; Lifson, S. *Ibid.* **1970,** *53*, 582. (c) Gelin, B. R.; Karplus, M. *J. Am. Chem. Soc.* **1975,** *97*, 6996.
(60) Warshel, A.; Karplus, M. *Chem. Phys. Lett.* **1975,** *32*, 11, and references cited therein.

(61) Miller, W. H.; George, T. F. J. Chem. Phys. 1972, 56, 5637.
(62) Birge, R. R.; Hubbard, L. M., to be published.
(63) Hubbard, L. M. Ph.D. Thesis, University of California, Riverside, 1980.
(64) Warshel, A.; Karplus, M. J. Am. Chem. Soc. 1974, 96, 5677.
(65) Excited-state lifetimes are determined by following trajectories until a fraction of less than e^{-1} (0.37) of the molecules remain in the excited state. Intrinsic isomerization times are determined by following trajectories until a fraction of more than $(1 - e^{-1})$ (0.63) of the molecules are in the ground state with less than 63% of their original vibrational energy.
(66) Dartnall, H. J. A. In "Handbook of Sensory Physiology", Springer-Verlag: West Berlin, 1972; Vol. v11/1, p. 122.
(67) Stuckelberg, E. C. G. Helv. Phys. Acta 1932, 5, 369.
(68) As noted by one referee, our calculations predict counterion-induced blue shifts very similar to those obtained in the cruder calculations of ref 8 where the counterion is treated as a point charge.
(69) Huppert, D.; Rentzepis, P. M.; Kliger, D. S. Photochem. Photobiol. 1977, 25, 193.
(70) Waddell, W. H.; Hopkins, D. L. J. Am. Chem. Soc. 1977, 99, 6458.

On Berry Pseudorotation in ML_5 Molecules and Microwave Dielectric Absorption

E. N. DiCarlo

Contribution from the Department of Chemistry, Saint Joseph's University, Philadelphia, Pennsylvania 19131. *Received March 19, 1979*

Abstract: The possibility of applying microwave dielectric relaxation to the study of an extremely rapid chemical rate process of the intramolecular rearrangement type has been explored. A dispersion investigation at temperatures between −10 and 30 °C and several frequencies within the range, 0.002–135 GHz, has been conducted on iron pentacarbonyl, $Fe(CO)_5$, which is known to undergo axial/equatorial internal ligand exchange at a rate that is much too fast to monitor by NMR methods and too slow for electronic or vibrational spectral techniques. The study shows that $Fe(CO)_5$, whose instantaneous structure is of D_{3h} symmetry and therefore nonpolar, exhibits significant microwave absorption in the range of 0.3–5 cm^{-1}. The present dielectric results, when considered in the light of previous nondielectric investigations, appear to be best explained in terms of a fluxional relaxation model involving very rapid interconversion of nonpolar and transiently polar configurations. In the context of the mechanism proposed, the temperature dependence of the observed relaxation is indicative of a very low activation energy, 1.9 ± 0.3 kcal mol^{-1}, for the ligand exchange process occurring in $Fe(CO)_5$. Tetraphenylantimony bromide, $(C_6H_5)_4SbBr$, which would not be anticipated to undergo facile intramolecular rearrangement, was also examined. Its relaxation behavior, in benzene solution at 25 °C, was found to be consistent with dielectric dispersion completely controlled by rotational diffusion of permanent molecular dipoles.

Recently,[1] it was shown that iron pentacarbonyl, $Fe(CO)_5$, exhibits significant microwave dielectric absorption in the range of 0.3–5 cm^{-1}. This observation was considered to be quite meaningful, particularly in reference to the dynamic nature of this molecule's structure since rotational absorption involving its "ground" vibrational state is forbidden by symmetry. The equilibrium configuration of $Fe(CO)_5$ is the trigonal bipyramid[2] (TBP, D_{3h} point group) and consequently is nonpolar. After a consideration of various mechanistic possibilities, the unusually high-frequency dispersion and the temperature coefficient of its associated relaxation time were qualitatively explained on the basis of this molecule's well-established fluxional nature.[1] Earlier ^{13}C NMR studies on $Fe(CO)_5$ found only one resonance line down to the lowest possible solution temperature even though two signals (3:2 ratio) would be expected for the TBP ground-state geometry, pointing to an extremely rapid exchange of carbonyl ligands between nonequivalent sites.[3] All known aspects of dynamical stereochemistry for $Fe(CO)_5$ and numerous other ML_5 complexes[4] (PF_5, $Sb(CH_3)_5$, AsF_5) which also show apparent magnetic equivalence of ligand nuclei are in accordance with the Berry pseudorotation (BPR) mechanism[5] or a permutational equivalent.[6] In the Berry rearrangement, TBP and square-pyramidal (SP) geometries are traversed via small angle deformation motions, thereby enabling two axial and two equatorial positions of the TBP to be simultaneously interchanged in a single step.[5,6] The inability to observe temperature coalescence of NMR spectral lines for $Fe(CO)_5$ (which is indicative of a very low barrier to internal ligand exchange) reflects, in terms of the classic Berry permutation process, a correspondingly small energy difference between the TBP and SP structures.[7]

The purpose of the present work is to demonstrate, via a simple relaxation model, that extremely rapid BPR in ML_5 molecules can, in principle, lead to a distinct microwave dielectric relaxation effect which directly reflects the dynamics of the chemical rate process. In addition, dielectric dispersion results obtained on a dipolar five-coordinate molecule, i.e., $(C_6H_5)_4SbBr$, which is expected to have a long ground-state lifetime, are reported and compared with those observed for fluxional $Fe(CO)_5$.

Discussion

The dielectric dispersion of $Fe(CO)_5$, as the pure liquid, was previously investigated at frequencies of 2 MHz, 9.2, 24.4, and 135 GHz,[1] and at several temperatures[8] between −10 and 30 °C. For the sake of clarity, the prominent features of the latter study will be briefly summarized. In general, the relaxation behavior at all of the temperatures investigated displays the same basic characteristics and appears to follow, well within the uncertainty of the data, a common form of the absorption curve. The −10 and 30 °C absorption results are depicted in Figure 1 on the basis of a Debye exponential decay function. Taking the 30 °C observations as an example, a contribution to the static polarization of ~0.4 cm^3 (corresponding to an effective moment of 0.14 D) dispersing according to the Debye form of the loss curve with a relaxation time, τ, of 1.0 ps accounts for the relaxation behavior. Although the present data are too limited to necessitate interpretation in terms of a single Debye-type relaxation, knowledge of the exact line shape of the absorption (requiring measurements at still higher frequencies) would not change the magnitude of the τ values to any appreciable extent and consequently would not alter the main point to be made.[9] Table I contains the pertinent end results derived from the frequency dependence of the dielectric losses, assuming a single Debye-type absorption.[10] From a

0002-7863/80/1502-2205$01.00/0